Journal for Geometry and Graphics
Volume 24 (2020), No. 1, 79–101.

The Ballet of Triangle Centers on the Elliptic Billiard

Dan S. Reznik[1], **Ronaldo Garcia**[2], **Jair Koiller**[3]

[1] *Data Science Consulting*
Rio de Janeiro RJ 22210-080, Brazil
email: dreznik@gmail.com

[2] *Instituto de Matemática e Estatística, Universidade Federal de Goiás, Goiânia GO, Brazil*
email: ragarcia@ufg.br

[3] *Universidade Federal de Juiz de Fora, Juiz de Fora MG, Brazil*
email: jairkoiller@gmail.com

Abstract. We explore a bevy of new phenomena displayed by 3-periodics in the Elliptic Billiard, including (i) their dynamic geometry and (ii) the non-monotonic motion of certain Triangle Centers constrained to the Billiard boundary. Fascinating is the *joint* motion of certain pairs of centers, whose many stops-and-gos are akin to a Ballet.

Key Words: elliptic billiard, periodic trajectories, triangle center, loci, dynamic geometry.

MSC 2010: 51N20, 51M04, 51-04, 37-04

1. Introduction

We investigate properties of the 1d family of 3-periodics in the Elliptic Billiard (EB). Being uniquely integrable [13], this object is the *avis rara* of planar Billiards. As a special case of Poncelet's Porism [4], it is associated with a 1d family of N-periodics tangent to a confocal Caustic and of constant perimeter [27]. Its plethora of mystifying properties has been extensively studied, see [26, 10] for recent treatments.

Initially we explored the loci of *Triangle Centers* (TCs): e.g., the Incenter X_1, Barycenter X_2, Circumcenter X_3, etc., see summary below. The X_i notation is after KIMBERLING's Encyclopedia [14], where thousands of TCs are catalogued. Here we explore a bevy of curious behaviors displayed by the family of 3-periodics, roughly divided into two categories (with an intermezzo):

1. The *shape* of 3-periodics and/or TC loci: when are the former acute, obtuse, pythagorean, and the latter non-smooth, self-intersecting, non-compact? See for example this recent treatment of TCs at infinity [15].

ISSN 1433-8157/$ 2.50

2. The *kinematics* of EB-railed TCs: a handful of TCs[1] is known to lie on the EB. As the family of 3-periodics is traversed, what is the nature of their motion (monotonicity, critical points, etc.). We further examine the *joint* motion of two EB-railed TCs which in some cases resembles a Ballet.

In the intermezzo we introduce (i) a deceptively simple construction under which the EB bugles out the Golden Ratio, and (ii) a triangle closely related to 3-periodics[2], whose vertices are dynamically clutched onto the EB.

Throughout the paper figures will sometimes include a hyperlink to an animation in the format [23, PL#nn], where nn is the entry into our video list on Table 5 in Section 5. Indeed, the beauty of most phenomena remain ellusive unless they are observed dynamically.

Related Work Properties of the *poristic* triangle family, i.e., one with fixed incircle and circumcircle, were studied in [29, 31, 18], where the loci of many triangle centers is described. Indeed, we noticed poristic triangles are related to the 3-periodic family by a variable similarity transform, therefore sharing with it all scale-free invariants [7].

Regarding 3-periodics, two intriguing invariants are [24]:

1. The Mittenpunkt X_9 is the black swan of all TCs: its locus is a *point* at the center of the EB[3] [23, PL#01].
2. The 3-periodic family conserves the ratio of Inradius-to-Circumradius. This implies the sum of its cosines is invariant. Suprisingly the latter holds for all N-periodics [1, 2].

Other observations focused on the surprising elliptic locus of many TCs: the locus of the Incenter X_1 is an ellipse [25], as is that of the Excenters [6]. The latter is similar to a rotated locus of X_1, see [23, PL#01,04]. Also elliptic are the loci of the Barycenter X_2 [28], Circumcenter X_3 [5], Orthocenter X_4 [6], Center X_5 of the Nine-Point Circle [8], see [23, PL#05,07]. Recently we showed that out of the first 100 Kimberling Centers in [14], exactly 29 produce elliptic loci [8]. This is quite unexpected given the non-linearities involved.

Other observations, many which find parallels in Triangle Geometry, included (i) the locus of the Feuerbach Point X_{11} is on the Caustic[4], as is that of the Extouchpoints, though these move in opposite directions; (ii) the locus of X_{100}, the anticomplement of X_{11}, is on the EB [9]; (iii) the locus of vertices of Intouch, Medial and Feuerbach Triangles are all non-elliptic.

We still don't understand how loci ellipticity or many of the phenomena below correlate to the Trilinears of a given TC.

2. First movement: shape

Let the boundary of the EB be given by, $a > b > 0$:

$$f(x,y) = \left(\frac{x}{a}\right)^2 + \left(\frac{y}{b}\right)^2 = 1 \tag{1}$$

Below $c^2 = a^2 - b^2$, and $\delta = \sqrt{a^4 - a^2b^2 + b^4}$.

[1] Some 50 out of 40 thousand in [14].

[2] The Contact (or Intouch) Triangle of the Anticomplementary Triangle (ACT).

[3] In Triangle parlance, the EB is the "X_9-Centered Circumellipse".

[4] The Inconic centered on the Mittenpunkt X_9 which passes through the Extouchpoints is known as the *Mandart Inellipse* [30]. By definition, an Inconic is internally tangent to the sides, so it must be the Caustic.

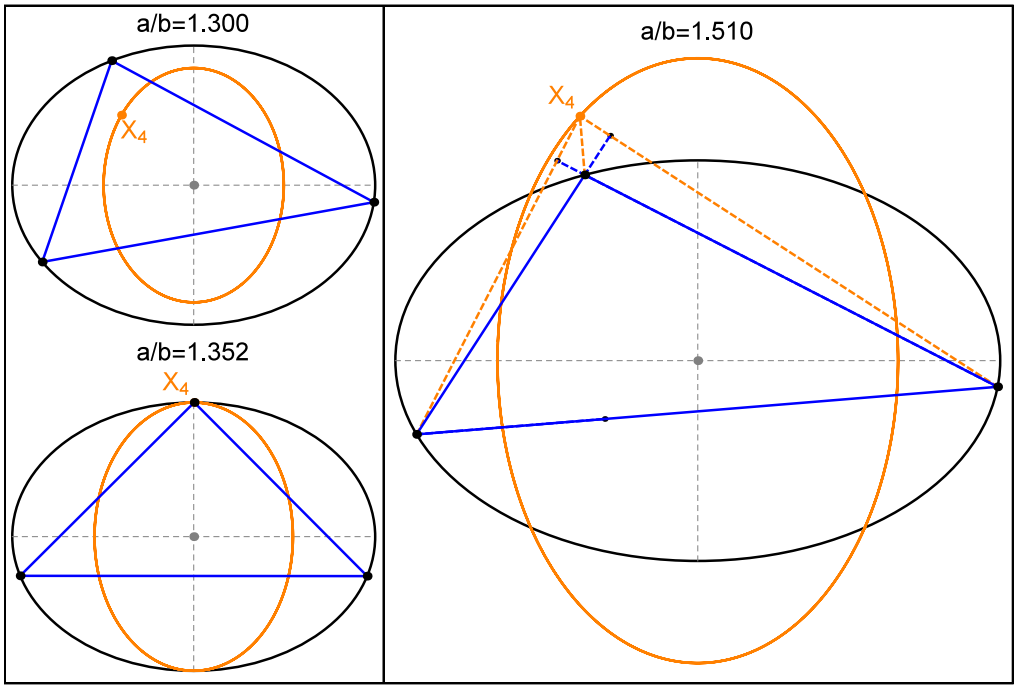

Figure 1: Let $\alpha_4 = \sqrt{2\sqrt{2}-1} \simeq 1.352$ and H be the elliptic locus of X_4 (orange), similar to a rotated copy of the EB (black). **Top Left**: $a/b < \alpha_4$, H is interior to the EB and all 3-periodics (blue) are acute. **Bot Left**: at $a/b = \alpha_4$, H is tangent to the top and bottom vertices of the EB. The 3-periodic shown is a right triangle since one vertex is at the upper EB vertex where X_4 currently is. **Right**: at $a/b > \alpha_4$, the 3-periodic family will contain both acute and obtuse 3-periodics, corresponding to X_4 interior (resp. exterior) to the EB. For any obtuse 3-periodic, X_4 will lie within the wedge between sides incident upon the obtuse angle and exterior to the 3-periodic, i.e., exterior to the EB. For the particular aspect ratio shown ($a/b = 1.51$), H is identical to a 90°-rotated copy of the EB.

Throughout this paper we assume one vertex $P_1(t) = (x_1, y_1)$ of a 3-periodic is parametrized as $P_1(t) = [a\cos t, b\sin t]$. Explicit expressions[5] for the locations of $P_2(t)$ and $P_3(t)$ under this specific parametrization are given in Appendix B.

2.1. Can 3-periodics be obtuse? Pythagorean?

The locus of the Orthocenter X_4 is an ellipse of axes a_4, b_4 similar to a rotated copy of the EB. These are given by [8]:

$$(a_4, b_4) = \left(\frac{k_4}{a}, \frac{k_4}{b}\right), \quad k_4 = \frac{(a^2+b^2)\delta - 2\,a^2b^2}{c^2}$$

Referring to Figure 1, let $\alpha_4 = \sqrt{2\sqrt{2}-1} \simeq 1.352$.

Proposition 1. *If $a/b = \alpha_4$, then $b_4 = b$, i.e., the top and bottom vertices of the locus of X_4 coincide with the EB's top and bottom vertices.*

[5] Their coordinates involve double square roots on x_1 so these points can be constructed by ruler and compass.

Proof. The equation $b_4 = b$ is equivalent to $a^4 + 2a^2b^2 - 7b^4 = 0$. Therefore, as $a > b > 0$, it follows that $a/b = \sqrt{2\sqrt{2} - 1}$. □

Let α_4^* be the positive root of $x^6 + x^4 - 4x^3 - x^2 - 1 = 0$, i.e., $\alpha_4^* = \simeq 1.51$.

Proposition 2. *When $a/b = \alpha_4^*$, then $a_4 = b$ and $b_4 = a$, i.e., the locus of X_4 is identical to a rotated copy of Billiard.*

Proof. The condition $a_4 = b$, or equivalently $b_4 = a$, is defined by $a^6 + a^4b^2 - 4a^3b^3 - a^2b^4 - b^6 = 0$. Graphic analysis shows that $x^6 + x^4 - 4x^3 - x^2 - 1 = 0$ has only one positive real root which we call α_4^*. □

Theorem 1. *If $a/b < \alpha_4$ (resp. $a/b > \alpha_4$) the 3-periodic family will not (resp. will) contain obtuse triangles.*

Proof. If the 3-periodic is acute, X_4 is in its interior, therefore also internal to the EB. If the 3-periodic is a right triangle, X_4 lies on the right-angle vertex and is therefore on the EB. If the 3-periodic is obtuse, X_4 lies on exterior wedge between sides incident on the obtuse vertex (feet of altitudes are exterior). Since the latter is on the EB, X_4 is exterior to the EB. □

2.2. Can a locus be non-smooth?

Loci considered thus far have been smooth, regular curves.

Proposition 3. *If $a/b > \alpha_4$ the locus of the Incenter of the 3-periodic's Orthic Triangle comprises four arcs of ellipses, connected at four corners.*

To see this, let T be a triangle, T_h its Orthic[6], and I_h be the latter's Incenter. It is well-known that if T is acute I_h coincides with T's Orthocenter X_4. However, for obtuse T:

Lemma 1. *T_h has two vertices outside of T, and I_h is "pinned" to the obtuse vertex.*

This is a known result [3, Chapter 1], which we revisit in Appendix A. This curious phenomenon is illustrated in Figure 2.

Assume $a/b > \alpha_4$. Since the 3-periodic family contains both acute and obtuse triangles, the locus of I_h transition between acute and obtuse regimes:

3-periodic	X_4 wrt EB	I_h location
acute	interior	Orthocenter X_4
right triangle	on it	right-angle vertex
obtuse	external (3-periodic Excenter)	obtuse vertex, on EB

In turn, this yields a locus for I_h consisting of four elliptic arcs connected by their endpoints in four corners (Figure 3). Notice top and bottom (resp. left and right) arcs belong to the EB (resp. X_4 locus).

For the next proposition, let α_h^2 (resp. $1/\alpha_h'^2$) be the real root above 1 (resp. less than 1) of the polynomial $1 + 12x - 122x^2 - 52x^3 + 97x^4$. Numerically, $\alpha_h \simeq 1.174$ and $\alpha_h' \simeq 2.605$.

Proposition 4. *At $a/b = \alpha_h$ (resp. $a/b = \alpha_h'$), at the sideways (resp. upright) 3-periodic, the Orthic is a right triangle (Figure 4). If $a/b > \alpha_h$ some Orthics are obtuse (a family always contains acutes).*

[6] Its vertices are the feet of the altitudes.

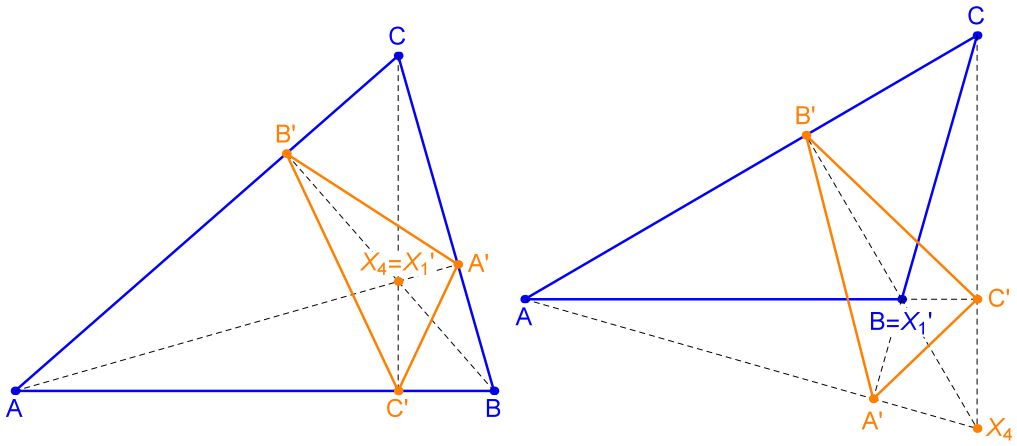

Figure 2: **Left**: If $T = ABC$ is acute (blue), its Orthic $T' = A'B'C'$ is the so-called Fagnano Triangle [26], whose properties include: (i) inscribed triangle of minimum perimeter, (ii) a 3-periodic of T, i.e., the altitudes of T are bisectors of T', i.e., the Orthic Incenter X_1' coincides with the Orthocenter X_4. **Right**: If T is obtuse, two of the Orthic's vertices lie outside T, and X_4 is exterior to T. T' is the Orthic of *both* T and *acute* triangle $T_e = AX_4C$. So the Orthic is the latter's Fagnano Triangle, i.e., B is where both altitudes and bisectors meet. The result is that if T is obtuse at B, the Incenter X_1' of the Orthic is B. **Video**: [23, PL#06]

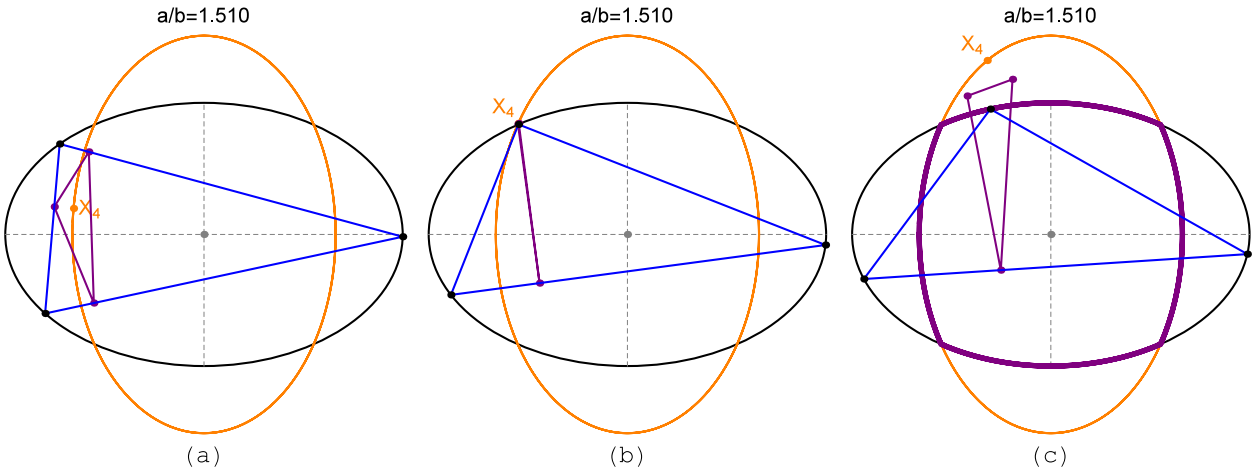

Figure 3: An $a/b > \alpha_4$ EB is shown (black). Let T and T_h be the 3-periodic and its Orthic Triangle (blue and purple, respectively). **(a)** T is acute (X_4 is interior to the EB), and $I_h = X_4$. **(b)** X_4 is on the EB and T is a right triangle. T_h degenerates to a segment. **(c)** X_4 is exterior to the EB. Two of T_h's vertices are outside T. I_h is pinned to T's obtuse vertex, on the EB. X_4 is an Excenter of the 3-periodic. The complete locus of I_h comprises therefore 4 elliptic arcs (thick purple) duck-taped at the corners. **Video**: [23, PL#07]

Proof. The orthic of an isosceles triangle with vertices $A = (a, 0)$, $B = (-u, v)$ and $C = (-u, -v)$ is the isosceles triangle with vertices:

$$
\begin{aligned}
A' &= (-u,\, 0) \\
B' &= \left(\frac{-u(a+u)^2 + v^2(2a+u)}{(a+u)^2 + v^2},\ \frac{v((a+u)^2 - v^2)}{(a+u)^2 + v^2} \right) \\
C' &= \left(\frac{-u(a+u)^2 + v^2(2a+u)}{(a+u)^2 + v^2},\ -\frac{v((a+u)^2 - v^2)}{(a+u)^2 + v^2} \right)
\end{aligned}
$$

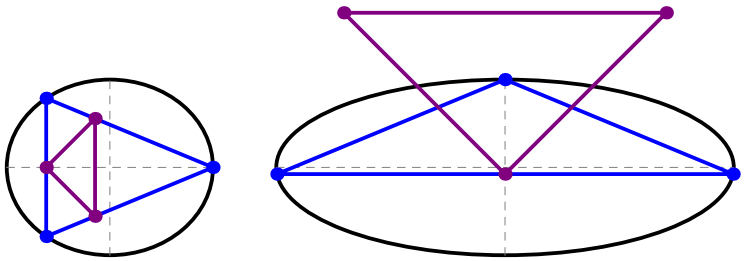

Figure 4: **Left**: At $a/b = \alpha_h \simeq 1.174$, a sideways 3-periodic (blue) has a right-triangle Orthic (purple). If $a/b > \alpha_h$ some Orthics in the family are obtuse. **Right**: At $a/b = \alpha'_h \simeq 2.605$, when the 3-periodic is an upright isosceles (obtuse since $a/b > \alpha_h$), its extraverted Orthic is also a right triangle.

It is rectangle, if and only if, $\langle B' - A', C' - A' \rangle = 0$. This condition is expressed by $r(a, u, v) = (a + u)^2 - v(2a + 2u + v) = 0$.

Using explicit expression to the 3-periodic vertices [6], obtain that $u = u(a, b) = a(\delta - b^2)/(a^2 - b^2)$ and $v = v(a, b) = b^2\sqrt{2\delta - a^2 - b^2}/(a^2 - b^2)$. So it follows that $r(a, u, \simeq) = r(a, b) = 97a^8 - 52a^6b^2 - 122a^4b^4 + 12a^2b^6 + b^8 = 0$. The same argument can be applied to the isosceles 3-periodic with vertices:

$$A = (0, b), \quad B = (-v(b, a), -u(b, a)), \quad C = (v(b, a), -u(b, a))$$

The associated orthic triangle will be rectangle, if and only if, $r(b, a) = 0$. □

The obtuseness of 3-periodic Orthics is a complex phenomenon with several regimes depending on a/b, beyond the scope of this paper. It is explored in [23, PL#08].

2.3. Can a locus be self-intersecting?

The trees are in their autumn beauty,
The woodland paths are dry,
Under the October twilight the water
Mirrors a still sky;
Upon the brimming water among the stones
Are nine-and-fifty swans.

W.B. Yeats

Yeats gave us the idea to look at a curious TC: X_{59}, the "Isogonal Conjugate of X_{11}" [14], i.e., the two centers have reciprocal trilinears.

Experimentally, X_{59} is a continuous curve internally tangent to the EB at its four vertices, and with four self-intersections (Figure 5), and as an animation [23, PL#12]. It intersects a line parallel to and infinitesimally away from either axis on six points, so its degree must be at least 6. Producing analytic expressions for salient aspects of its geometry has proven a tough nut to crack, namely, the following are unsolved:

- What is the degree of its implicit equation?
- What is t in $P_1(t) = (a\cos(t), b\sin(t))$ such that X_{59} is on one of the four self-intersections? For example, at $a/b = 1.3$ (resp. 1.5), t, given in degrees is $\simeq 32.52°$ (resp. 29.09°) (Figure 5, left-bottom).
- What is a/b such that if X_{59} is on one of the lower self-intersection on the y-axis, the 3-periodic is a right triangle? Numerically, this occurs when $a/b = \alpha_{59}^{\perp} \simeq 1.58$ and $t \simeq 27.92°$ (Figure 5, right).

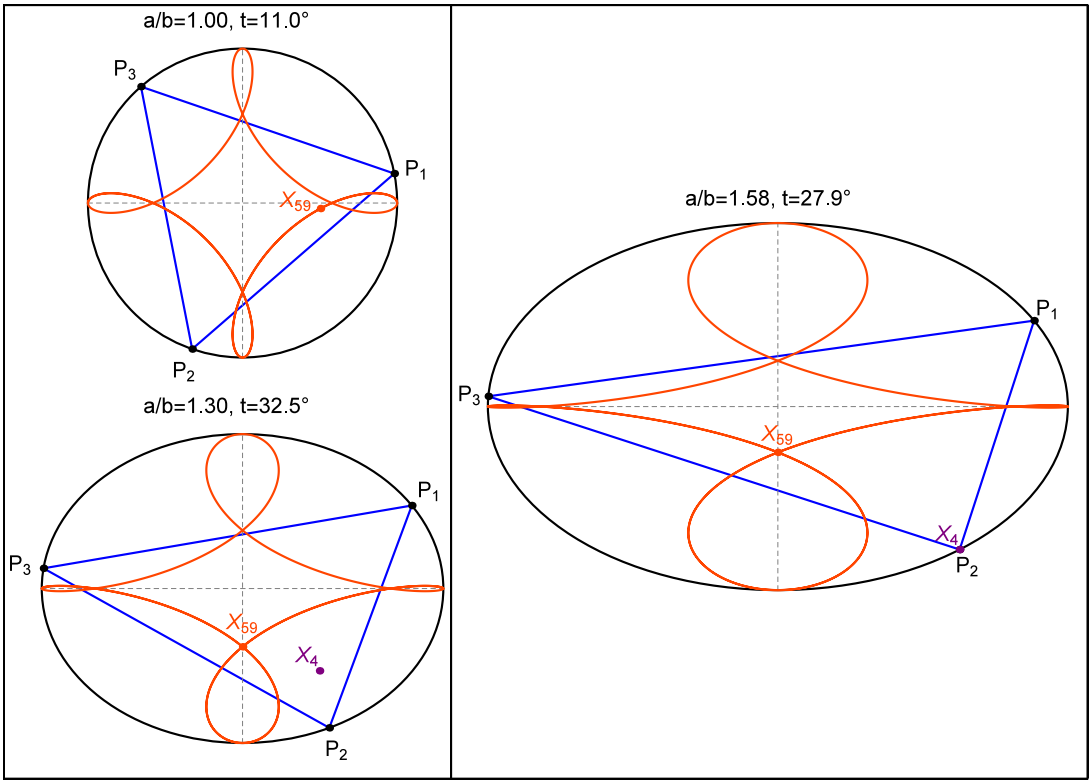

Figure 5: The locus of X_{59} is a continuous curve with four self-intersections, and at least a sextic. It is tangent to the EB at its four vertices. **Top Left**: circular EB, X_{59} is symmetric about either axis. **Bottom Left**: $a/b = 1.3$, at $t{\simeq}32.5°$ X_{59} is at the lower self-intersection and the 3-periodic is acute (X_4 is interior). **Right**: at $a/b = \alpha_{59}^{\perp} \simeq 1.58$ the following feat is possible: X_{59} is at the lower self-intersection *and* the 3-periodic is a right-triangle (X_4 is on P_2). This occurs at $t{\simeq}27.9°$. **Video**: [23, PL#12]

2.4. Can a locus be non-compact

X_{26} is the Circumcenter of the Tangential Triangle [30]. Its sides are tangent to the Circumcircle at the vertices. If the 3-periodic is a right-triangle, its hypotenuse is a diameter of the Circumcircle, and X_{26} is unbounded.

We saw above that:

- $a/b < \alpha_4$, the 3-periodic family is all-acute, i.e., the locus of X_{26} is compact (Figure 1, top left).
- $a/b = \alpha_4$, the family is all-acute except when one of its vertices coincides with the top or bottom vertex of the EB (Figure 1, bottom left). In this case the 3-periodic is a right triangle and X_{26} is unbounded.
- $a/b > \alpha_4$, the family features both acute and obtuse triangles. The transition occurs at for four right-angle 3-periodics whose X_4 is on the EB (Figure 3(b)). Here too X_{26} flies off to infinity (Figure 6).

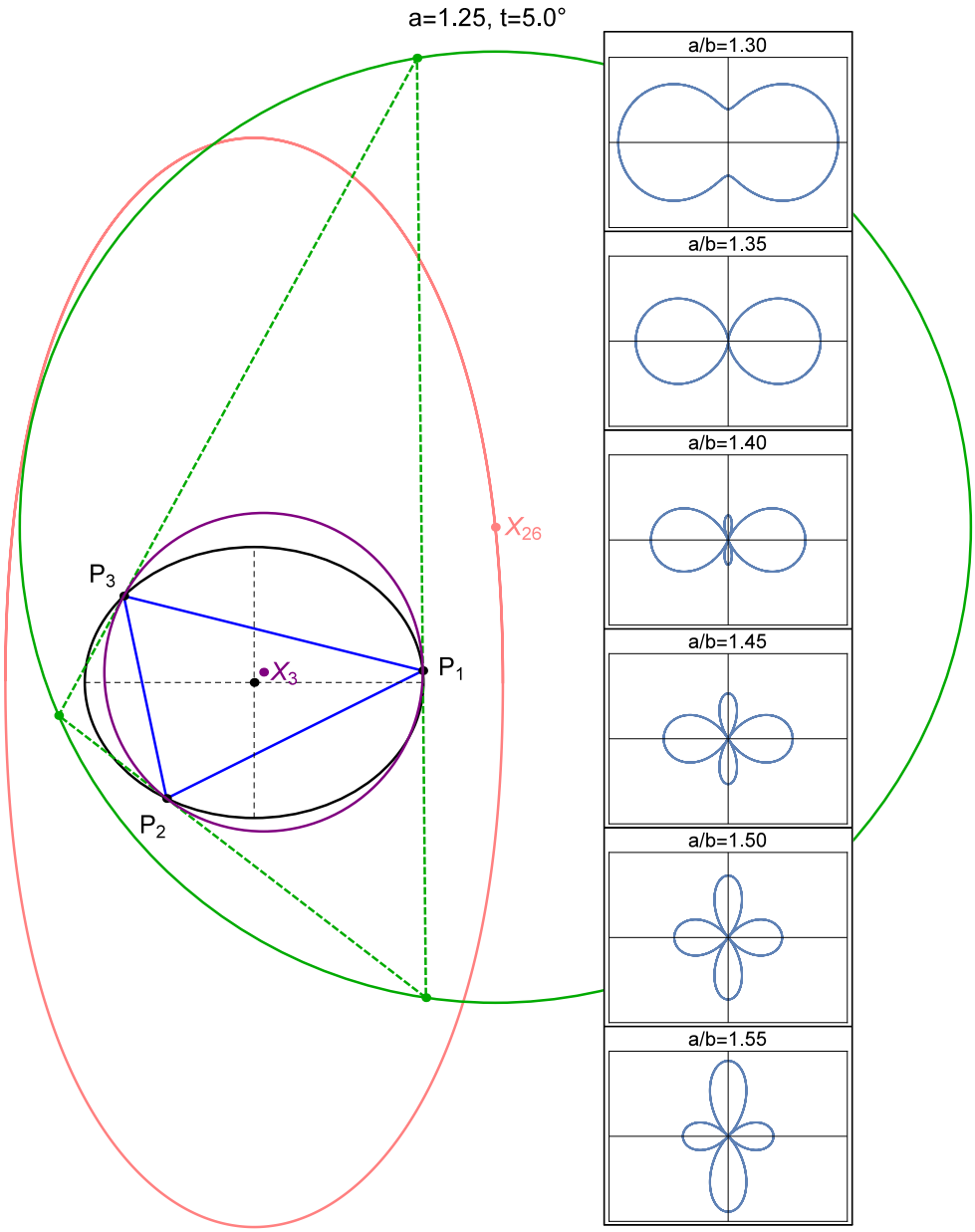

Figure 6: The locus of X_{26} for a 3-periodic (blue) in an $a/b = 1.25$ EB (black). Also shown is the 3-periodic's Circumcircle (purple) and its Tangential Triangle [30] (dashed green). X_{26} is the center of the latter's Circumcircle (solid green). Its locus is non-elliptic. In fact, when $a/b \geq \alpha_4$, the 3-periodic family will contain right-triangles (X_4 crosses the EB). At these events, X_{26} flies off to infinity. The right inset shows an inversion of X_{26} with respect to the EB center for various values of a/b. When $a/b > \alpha_4$, the inversion goes through the origin, i.e., X_{26} is at infinity.

3. Intermezzo: Two unexpected phenomena

3.1. The billiard lays a golden egg

The *Bevan Point* X_{40} is known as the Circumcenter of the Excentral Triangle [14]. It is the tangential polygon to the 3-periodic, and can be thought of as its projective dual [17].

We have shown elsewhere the locus of X_{40} is an ellipse similar to a rotated copy of the

Billiard. Its semi-axes are given by [8]:

$$a_{40} = c^2/a, \quad b_{40} = c^2/b.$$

Proposition 5. *At $a/b = \sqrt{2}$ i.e., the top and bottom vertices of the X_{40} touch the Billiard's top and bottom vertices.*

Proof. This follows from imposing $b_{40} = b$. □

What we got next was unexpected (see Figure 7):

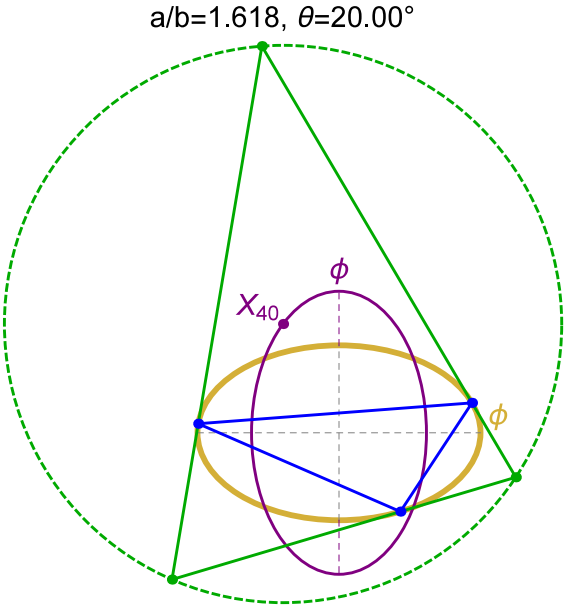

Figure 7: An $a/b = \varphi$ EB is shown golden. Also shown is a sample 3-periodic (blue). The Bevan Point X_{40} is the Circumcenter of the Excentral Triangle (solid green). At this EB aspect ratio, the locus of X_{40} (purple) is a 90°-rotated copy of the EB. The region common to both ellipses is ≃70.48% the area of either ellipse. **Video**: [23, PL#13].

Proposition 6. *At $a/b = (1+\sqrt{5})/2 = \varphi$, the Golden Ratio, the locus of X_{40} is identical to a 90°-rotated copy of the EB*

Proof. This follows from imposing $b_{40} = a$. □

Remark 1. Let A be area of the four-corner region common to an ellipse and its 90°-rotated copy. It can be shown $A/A_{ell} = 4\csc^{-1}\left[\sqrt{1+(a/b)^2}\right]/\pi$, where $A_{ell} = \pi ab$, is the area of the ellipse. For $a/b = \varphi$, $A/A_{ell} \simeq 0.704833$.

3.2. A derived triangle railed onto the EB

Consider a 3-periodic's Anticomplementary Triangle (ACT) [30] and its Intouchpoints i'_1, i'_2, i'_3 (Figure 8). Remarkably:

Theorem 2. *The locus of the Anticomplementary Triangle's Intouchpoints is the EB.*

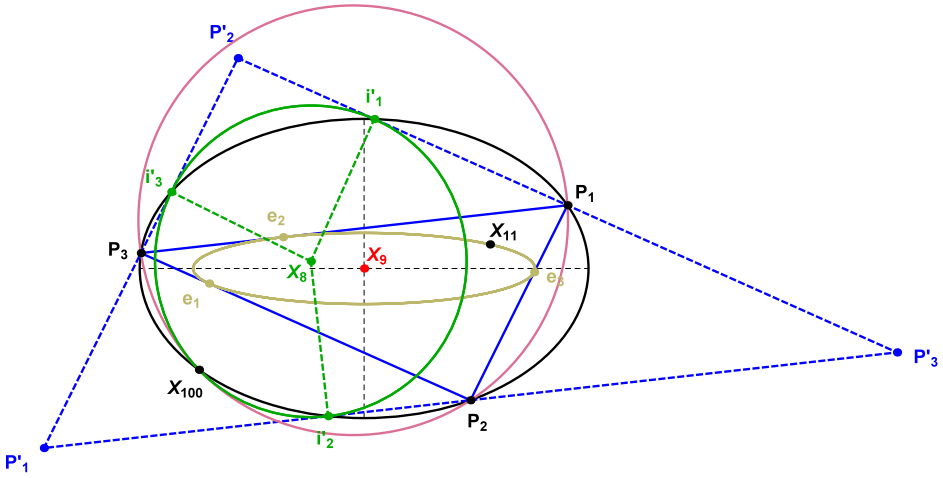

Figure 8: A 3-periodic $P_1P_2P_3$ is shown (blue). Shown also is the Mittenpunkt X_9, at the EB center. The 3-periodic's Anticomplementary Triangle (ACT) $P_1'P_2'P_3'$ (dashed blue) has sides parallel to the 3-periodic. The latter's Intouchpoints i_1', i_2', and i_3' are the feet of perpendiculars dropped from the ACT's Incenter (X_8) to each side (dashed green). The ACT's Incircle (green) and 9-point circle (the 3-periodic's Circumcircle, pink) meet at X_{100}, the ACT's Feuerbach Point. Its locus is also the EB. The Caustic is shown brown. On it there lie X_{11} and the three Extouchpoints e_1, e_2, e_3. **Video:** [23, PL#09]

Proof. Consider an elementary triangle with vertices $Q_1 = (0,0)$, $Q_2 = (1,0)$ and $Q_3 = (u,v)$. Its sides are $s_1 = |Q_3 - Q_2|$, $s_2 = |Q_3 - Q_1|$, and $s_3 = 1$.

Let E be its *Circumbilliard*, i.e., the Circumellipse for which $Q_1Q_2Q_3$ is a 3-periodic EB trajectory. The following implicit equation for E was derived [6]:

$$\begin{aligned} E(x,y) = &v^2x^2 + (u^2 + (s_1 + s_2 - 1)u - s_2)y^2 + \\ &v(1 - s_1 - s_2 - 2u)xy + v(s_2 + u)y - v^2x = 0 \end{aligned}$$

The vertices of the ACT are given by $Q_1' = (u-1, v)$, $Q_2' = (u+1, v)$, $Q_3' = (1-u, -v)$, and its Incenter[7] is:

$$X_1' = \left[s_1 - s_2 + u,\ \frac{s_2(s_1 - 1) + (1 - s_1 + s_2)u - u^2}{v} \right].$$

The ACT Intouchpoints are the feet of perpendiculars dropped from X_1' onto each side of the ACT, and can be derived as:

$$\begin{aligned} i_1' &= \left[\frac{s_1(u-1)u + s_2}{s_2}, \frac{v(s_1 - 1)}{s_2} \right], \\ i_2' &= \left[\frac{(u-1)(s_2 - 1)}{s_2}, \frac{(s_2 - 1)v}{s_2} \right], \\ i_3' &= [s_1 - s_2 + u, v]. \end{aligned}$$

Direct calculations shows that $E(i_1') = E(i_2') = E(i_3') = 0$. Besides always being on the EB, the locus of the Intouchpoints cover it. Let $P_1(t)P_2(t)P_3(t)$ be a 3-periodic and $P_1'(t)P_2'(t)P_3'(t)$ its ACT. For all t the Intouchpoint $i_1'(t)$ is located on the side $P_2'(t)P_3'(t)$ of the ACT and on the elliptic arc $\mathrm{arc}(P_1(t)P_3(t))$ (Figure 8). Therefore, when $P_1(t)$ completes a circuit on the EB, $i_1'(t)$ will have to complete a similar tour. Analogously for $i_2'(t)$ and $i_3'(t)$. □

[7] This is the Nagel Point X_8 of the original triangle.

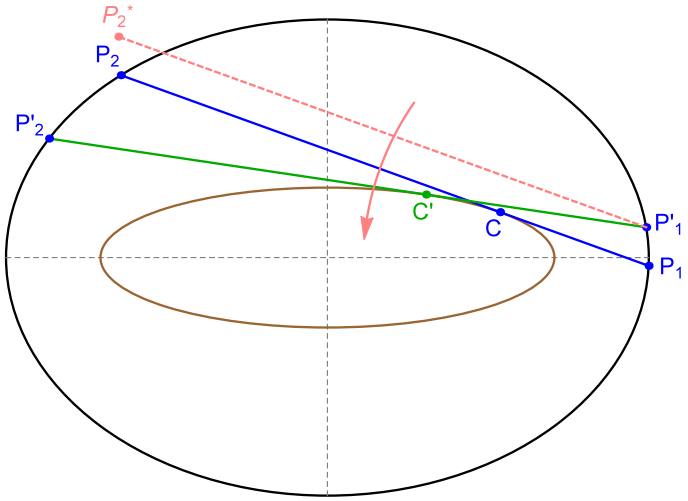

Figure 9: As one endpoint P_1 of a billiard trajectory is slid CCW to P_1', its tangency point C with the Caustic (brown) slides in the same direction to C'. This must be the case since $P_1'P_2'$ corresponds to a CCW rotation about P_1' of segment $P_1'P_2^*$ (pink) parallel to P_1P_2 (see pink arrow). By convexity, said rotation will first touch the Caustic at C', lying "ahead" of C. Repeating this for the P_2P_3 segment of a 3-periodic (not shown), it follows said vertices will move in the direction of P_1.

4. Second movement: motion

Let P_1, P_2, P_3 be the vertices of a 3-periodic (Appendix B).

Proposition 7. *If P_1 is slid along the EB in some direction, P_2 and P_3 will slide in the same direction.*

Proof. Consider the tangency point C of P_1P_2 with the confocal Caustic (Figure 9). Since this segment remains tangent to the Caustic for any choice of $P_1(t)$, a counterclockwise motion of $P_1(t)$ will cause C to slide along the Caustic in the same direction, and therefore $P_2(t)$ will do the same. □

The simultaneous monotonic motion of 3-periodic vertices is shown in Figure 10, note the non-linear progress of P_2, P_3. Alternatively, we could have linearized their motion using the

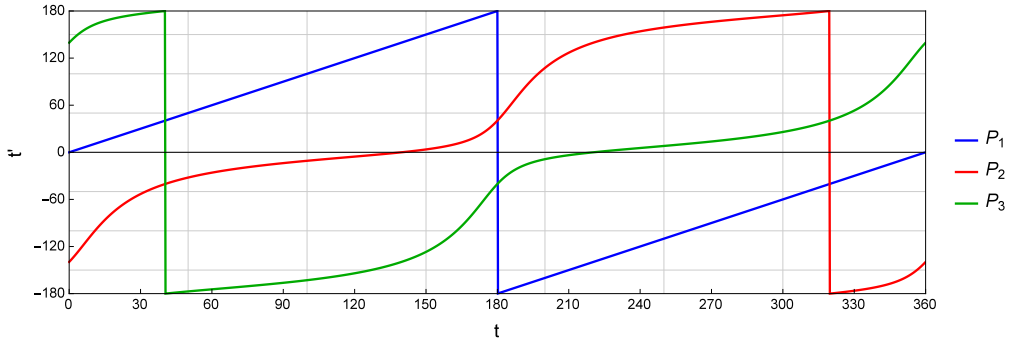

Figure 10: As $P_1(t)$ moves monotonically forward, so do $P_2(t)$ and $P_3(t)$, albeit with varying velocities with respect to t. In the text we mention an alternate parametrization (Poritsky-Lazutkin) under which the three lines would become straight.

so-called Poritsky-Lazutkin string length parameter η for C on the Caustic (Figure 9) given by [19, 16, 11]:

$$d\eta = \kappa^{2/3}\, ds,$$

where s is the arc length along the Caustic, and κ is the curvature. Both η and s are related to the parameter t on the billiard by elliptic functions. Adjusting conveniently with a constant factor, one has $\eta \equiv \eta + 1$ and for any η_o the other vertices correspond to $\eta_o + 1/3$ and $\eta_o + 2/3$.

4.1. Non-monotonicity: a first brushing

Let $\alpha_{act} = 2\sqrt{2/5} \simeq 1.2649$.

Proposition 8. *The motion of the ACT Intouchpoints is as follows:*

- $a/b < \alpha_{act}$*: monotonic in the direction of* $P_1(t)$*.*
- $a/b = \alpha_{act}$*: monotonic in the direction of* $P_1(t)$*, except for two instantaneous stops when passing at EB top and bottom vertices.*
- $a/b > \alpha_{act}$*: non-monotonic with four reversals of velocity, a first (resp. second) pair of reversals near the EB's top (resp. bottom) vertex (Figure 8).*

Proof. As before, let a 3-periodic $P_1P_2P_3$ be parametrized by a leading vertex

$$P_1(t) = (x_1, y_1) = (a\cos t,\, b\sin t).$$

Its ACT P_i' is given by double-length reflections of P_i about the Barycenter X_2 [30]. Taking the ACT as the reference triangle, use Intouchpoint Trilinears $0 : s_1 s_3/(s_1 - s_2 + s_3)$ :: [30, Contact Triangle] to compute an Intouchpoint $i_1'(t) = (x_1(t), y_1(t))$ it follows that $x_1'(t)\ |_{t=\frac{\pi}{2}} = 0$ is equivalent to $5a^2 - 8b^2 = 0$. This yields the result. □

See [22, PL#09] for an animation of the non-monotonic case. As we had been observing the EKG-like graph in Figure 11 (right), we stumbled upon an unexpected property, namely, the fixed linear relation between a 3-periodic vertex and its corresponding (opposite) Extouchpoint:

Proposition 9. *Let* $P_i(t) = (x_i, y_i)$ *be one of the 3-periodic vertices and* $e_i = (x_i', y_i')$ *be its corresponding Extouchpoint*[8] *on the Caustic, where* a_c, b_c *are the latter's semi-axes. Then*[9]*, for all* t*:*

$$\frac{a}{b}\frac{y_i}{x_i} = \frac{a_c}{b_c}\frac{y_i'}{x_i'} \tag{2}$$

Equivalently, for $e_i(t') = [a_c\cos t',\, b_c \sin t']$*, then* $\tan(t) = \tan(t')$*, i.e.,* $t' = t \pm \pi$*.*

Proof. This property follows directly[10] from [17, Lemma 3]. □

In fact, more general properties of the "Poncelet grid" are described in the reference above. The result reported here is a particular case and can also be demonstrated by simplifying rather long symbolic parametrics with a Computer Algebra System (CAS).

Furthermore, since $a_c = (\delta - b^2)a/c^2$ and $b_c = (a^2 - \delta)b/c^2$ [9]:

$$\frac{y}{x} = \left(\frac{\delta - b^2}{a^2 - \delta}\right)\frac{y'}{x'} \tag{3}$$

[8] Where $P_{i-1}(t)P_{i+1}(t)$ touch the Caustic.

[9] It can be shown (2) also holds if x', y' are the coordinates of an Excenter and a_c, b_c are the semi-axes of the excentral locus, known to be an ellipse [6].

[10] We thank A. Akopyan for pointing this out.

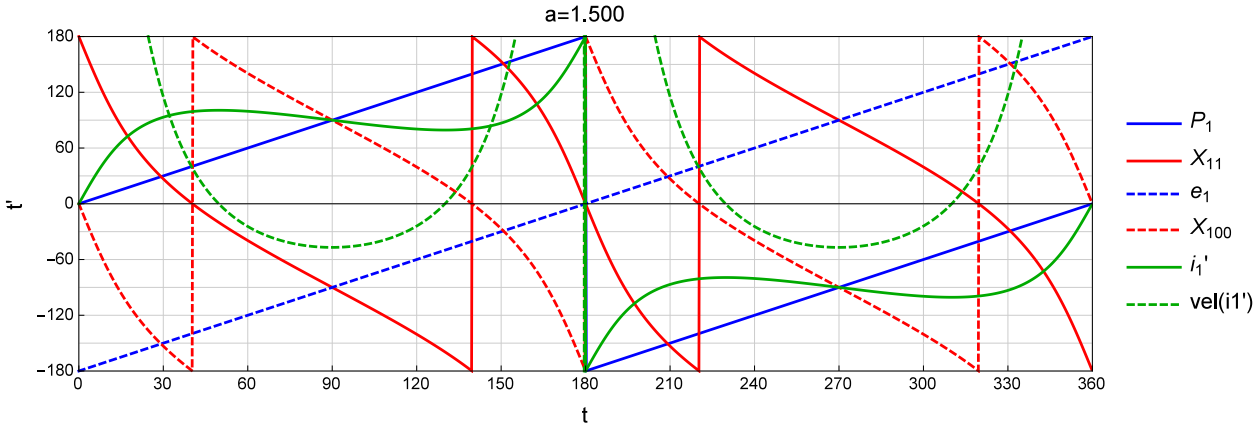

Figure 11: The "EKG" of ACT motion, to be interpreted as a flat torus. On the horizontal axis is parameter t of $P_1(t) = [a\cos(t), b\sin(t)]$, with $a/b = 1.5$. On the vertical is the t parameter for P_1, X_{11}, X_{100} and an ACT Intouchpoint i_1'. These all lie on the EB and are shown blue, red, dashed red, and green, respectively. Also shown is Extouchpoint e_1 on the Caustic (dashed blue). Just for it, the vertical axis represents t' in $e_1 = [a_c\cos(t'), b_c\sin(t')]$, where a_c, b_c are the Caustic semi-axes. By Proposition 9, $t' = t \pm \pi$. Notice the only non-monotonic motion is that of i_1' since $a/b > \alpha_{act} \simeq 1.265$. To see this, a vel$(i_1')$ of its velocity is also shown (dashed green), containing two negative regions corresponding to 4 critical points of position. For $vel(i_1')$ ignore units and the fact that values near $0°, 180°$ are not shown, these are all positive and above the vertical scale.

4.2. A non-monotonic triangle center

Dovetailing into the non-monotonicity of the ACT's Intouchpoints is a similar behavior by X_{88}, the Isogonal Conjugate of X_{44}, known to lie on the EB and to be collinear with X_1 and X_{100} [14]. The latter is verified by the vanishing determinant of the 3×3 matrix whose rows are the trilinears of X_1, X_{100}, X_{88} [30, under "Collinear", eqn 9]:

$$\det \begin{bmatrix} 1 & 1 & 1 \\ \dfrac{1}{s_2 - s_3} & \dfrac{1}{s_3 - s_1} & \dfrac{1}{s_1 - s_2} \\ \dfrac{1}{s_2 + s_3 - 2\,s_1} & \dfrac{1}{s_1 + s_3 - 2\,s_2} & \dfrac{1}{s_1 + s_2 - 2\,s_3} \end{bmatrix} \equiv 0$$

Furthermore X_{100} is a very special point: it lies on the EB and on the Circumcircle simultaneously [14]. Let $\alpha_{88} = (\sqrt{6 + 2\sqrt{2}})/2 \simeq 1.485$.

Proposition 10. *At $a/b = \alpha_{88}$, the y velocity of X_{88} vanishes when the 3-periodic is a sideways isosceles.*

Proof. Parametrize $P_1(t)$ in the usual way. At $t = 0$, $P_1 = (a, 0)$ it can be easily checked that $X_{88} = (-a, 0)$. Solve $y'_{88}(t)|_{t=0} = 0$ for a/b. After some algebraic manipulation, this is equivalent to solving $4x^4 - 12x^2 + 7 = 0$, whose positive roots are $(\sqrt{6 \pm 2\sqrt{2}})/2$. α_{88} is the largest of the two. □

As shown in Table 1, there are three types of X_{88} motion with respect to $P_1(t)$: monotonic, with stops at the EB vertices, and non-monotonic.

An equivalent statement is that the line family X_1X_{100} is instantaneously tangent to its *envelope* [30] at X_{88}. Figure 12 shows that said envelope lies (i) entirely inside, (ii) touches at

Table 1: Conditions for the type of motion of X_{88} with respect to $P_1(t)$. **Video**: [23, PL#11]

a/b vs. α_{88}	*motion*	*comment*
$<$	CW	monotonic
$=$	CW	stops at EB vertices
$>$	CW+CCW	non-monotonic

vertices of, or (iii) is partially outside, the EB, when a/b is less than, equal, or greater than α_{88}, respectively. Each such case implies the motion of X_{88} is (i) monotonically opposite to $P_1(t)$, (ii) opposite but with stops at the EB vertices, or (iii) is non-monotonic.

The reader is challenged to find an expression for parameter t in $P_1(t)$ where the motion

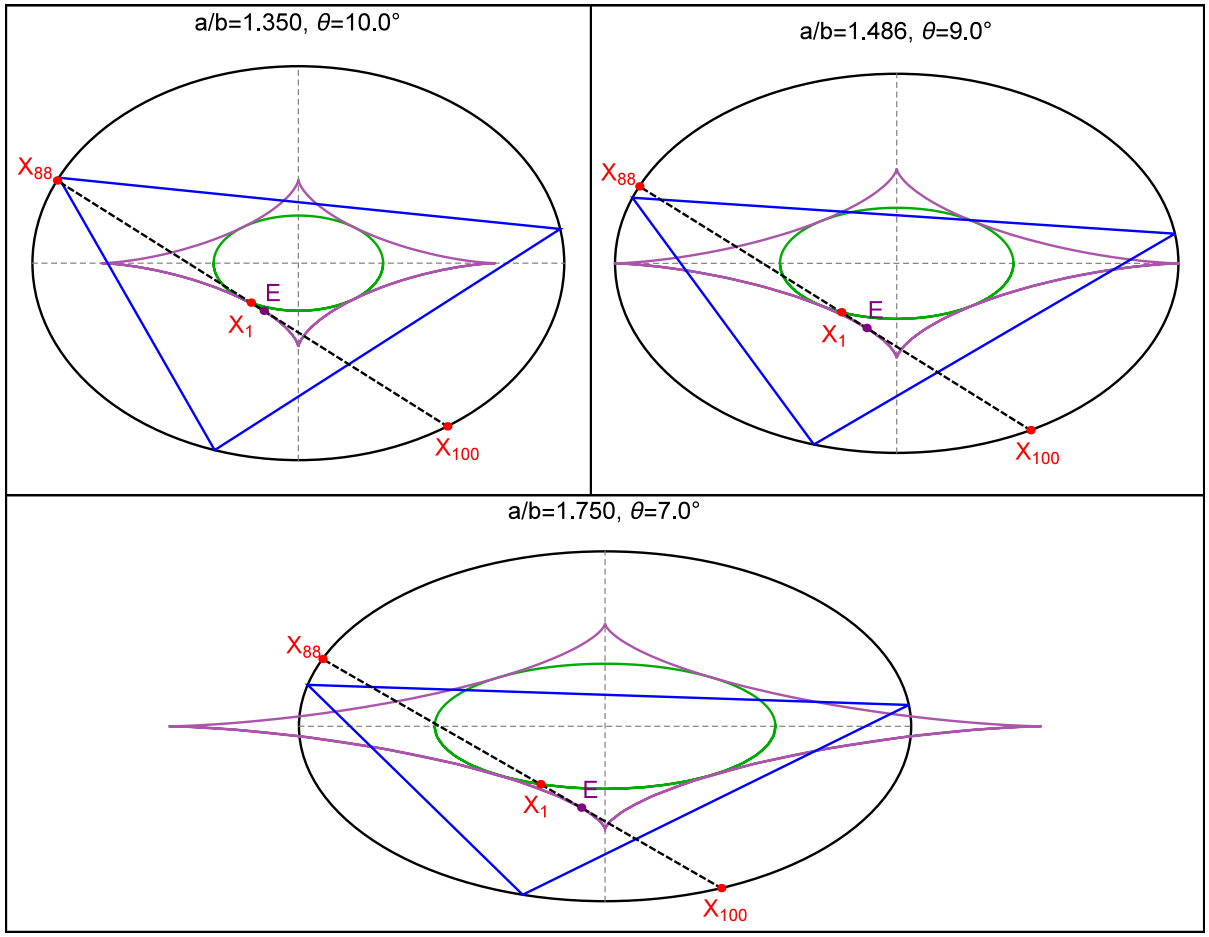

Figure 12: Collinear points X_1, X_{100}, X_{88} shown for billiards with a/b less than (top-left), equal (top-right), or greater (bottom) than $\alpha_{88}\simeq 1.486$, respectively. In each such case, the motion of X_{88} relative to the 3-periodic vertices will be monotonic, with stops at the vertices, or non-monotonic, respectively. Equivalently, the motion of X_{88} is opposite to P_1, stationary, or in the direction of P_1 if the instantaneous center of rotation E of line X_1X_{100} lies inside, on, or outside the EB. The locus of E (the envelope of X_1X_{100}) is shown purple. Notice it only "pierces" the EB when $a/b > \alpha_{88}$ (bottom), i.e., only in this case can the motion of X_{88} be non-monotonic. **Video**: [23, PL#12]

of X_{88} changes direction. The following additional facts are also true for X_{88}:

Proposition 11. *X_{88} coincides with a 3-periodic vertex if and only if $s_2 = (s_1 + s_3)/2$. In this case, X_1 is the midpoint between X_{100} and X_{88} [12] (Figure 13, bottom left).*

Proof. The first trilinear coordinate of X_{88} is $1/(s_2 + s_3 - 2s_1)$ [14], and of a vertex is 0. Equating the two yields $s_2 = (s_1 + s_3)/2$. Consider a triangle of reference $P_1 = (-1, 0)$, $P_2 = (u, v)$, $P_3 = (1, 0)$. Its circumcircle is given by $v(x^2+y^2)+(1-u^2-v^2)y-v = 0$. Under the hypothesis $s_2 = (s_1 + s_3)/2$ it follows that $v = \sqrt{12 - 3u^2}/2$, $s_1 = 2 - u/2$, $s_2 = 2$ and $s_3 = 2 + u/2$. Therefore the incenter is

$$I = (s_1P_1 + s_2P_2 + s_3P_3)/(s_1 + s_2 + s_3) = (u/2, \sqrt{12 - 3u^2}/6).$$

The intersection of the straight line passing through P_2 and I with the circumcircle of the triangle o reference is the point $D = (0, \sqrt{12 - 3u^2}/6)$. Therefore, I is the midpoint of B and $D = X_{100}$. Moreover, $|P_1 - D| = |P_2 - D| = |I - D| = \sqrt{48 - 3u^2}/6$. □

It is well-known that the only right-triangle with one side equal to the average of the other two is $3 : 4 : 5$. Let $\alpha_{88}^{\perp} = (7 + \sqrt{5})\sqrt{11}/22 \simeq 1.3924$. Referring to Figure 13 (right):

Proposition 12. *The only EB which can contain a 3:4:5 3-periodic has an aspect ratio $a/b = \alpha_{88}^{\perp}$.*

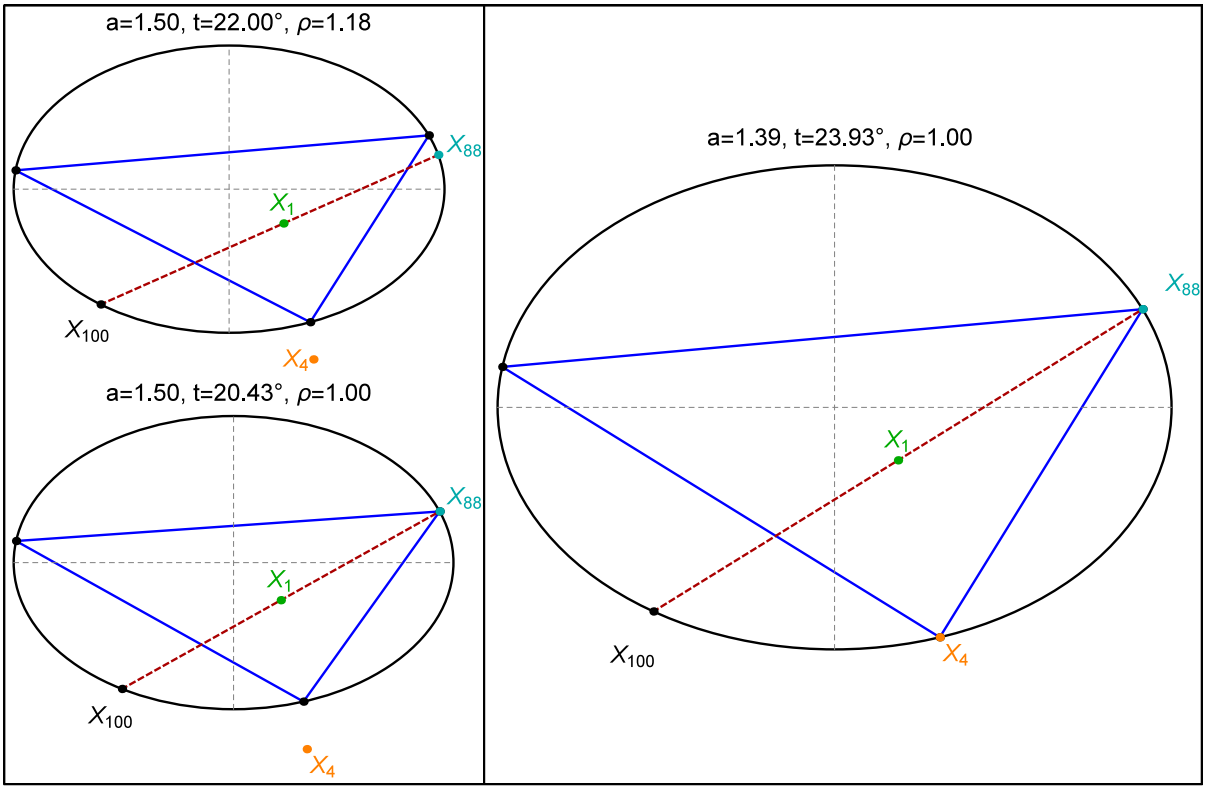

Figure 13: X_{88} is always on the EB and collinear with X_1 and X_{100} [14]. Let ρ (shown above each picture) be the ratio $|X_1 - X_{100}|/|X_1 - X_{88}|$. **Top Left**: The particular 3-periodic shown is obtuse (X_4 is exterior), and $\rho > 1$, i.e., X_1 is closer to X_{88}. **Bottom Left**: When X_{88} coincides with a vertex, if sidelengths are ordered as $s_1 \leq s_2 \leq s_3$, then $s_2 = (s_1 + s_3)/2$, and X_1 becomes the midpoint of $X_{88}X_{100}$, i.e., $\rho = 1$. **Right**: If $a/b = \alpha_{88}^{\perp} \simeq 1.39$, when X_{88} is on a vertex, the 3-periodic is a $3 : 4 : 5$ triangle (X_4 lies on an alternate vertex). **Video**: [23, PL#11]

Proof. With $a/b > \alpha_4 = \sqrt{2\sqrt{2}-1} \simeq 1.352$ the 3-periodic family contains obtuse triangles amongst which there always are 4 right triangles (identical up to rotation and reflection). Consider the elementary triangle $P_1 = (0,0)$, $P_2 = (s_1, 0)$, and $P_3 = (s_1, s_2)$ choosing s_1, s_2 integers such that $s_3 = s_3 = \sqrt{s_1^2 + s_2^2}$ is an integer. The Circumbilliard [9] is given by:

$$E_9(x,y) = s_2x^2 + (s_3 - s_1 - s_2)xy + s_1y^2 - s_1s_2x - s_1(s_1 - s_3)y = 0.$$

Squaring the ratio of the Eigenvalues of E_9's Hessian yields the following expression for a/b:

$$[a/b](s_1,s_2,s_3) = \frac{s_1 + s_2 + \sqrt{s_3\,(3\,s_3 - 2\,s_1 - 2\,s_2)}}{\sqrt{(s_1 + s_2 + 3\,s_3)\,(s_1 + s_2 - s_3)}}$$ □

Table 2 shows a/b for the first 5 Pythagorean triples ordered by hypotenuse[11].

Table 2: First 5 Pythagorean triples ordered by hypotenuse. a/b is the aspect ratio. of the EB which produces 4 triangles homothetic to the triple.

(s_1, s_2, s_3)	a/b	$\simeq a/b$
$3, 4, 5$	$(7+\sqrt{5})\sqrt{11}/22$	1.392
$5, 12, 13$	$\sqrt{14}(\sqrt{65}+17)/56$	1.674
$8, 15, 17$	$\sqrt{111}(\sqrt{85}+23)/222$	1.529
$7, 24, 25$	$\sqrt{159}(5\sqrt{13}+31)/318$	1.944
$20, 21, 29$	$\sqrt{6}(\sqrt{145}+41)/96$	1.353

4.3. Swan Lake

> But now they drift on the still water,
> Mysterious, beautiful;
> Among what rushes will they build,
> By what lake's edge or pool
> Delight men's eyes when I awake some day
> To find they have flown away?
>
> W.B. Yeats

In addition to X_{88} and X_{100}, a gaggle of 50+ other TCs are also known to lie on the EB [14, X(9)], e.g., X_{162}, X_{190}, X_{651}, etc. We have found experimentally that the motion of X_{100} and X_{190} is always monotonic.

In contradistinction: Let $\alpha_{162} \simeq 1.1639$ be the only positive root of $5x^8 + 3x^6 - 32x^4 + 52x^2 - 36$.

Proposition 13. *The motion of X_{162} with respect to $P_1(t)$ is non-monotonic if $a/b > \alpha_{162}$.*

Proof. The trilinear coordinates of X_{162} are given by

$$\frac{1}{(s_2^2 - s_3^2)(s_2^2 + s_3^2 - s_1^2)} : \frac{1}{(s_3^2 - s_1^2)(s_3^2 + s_1^2 - s_2^2)} : \frac{1}{(s_1^2 - s_2^2)(s_1^2 + s_3^2 - s_3^2)}\,.$$

[11] The a/b which produces $3:4:5$ was first computed in connection with X_{88} [12].

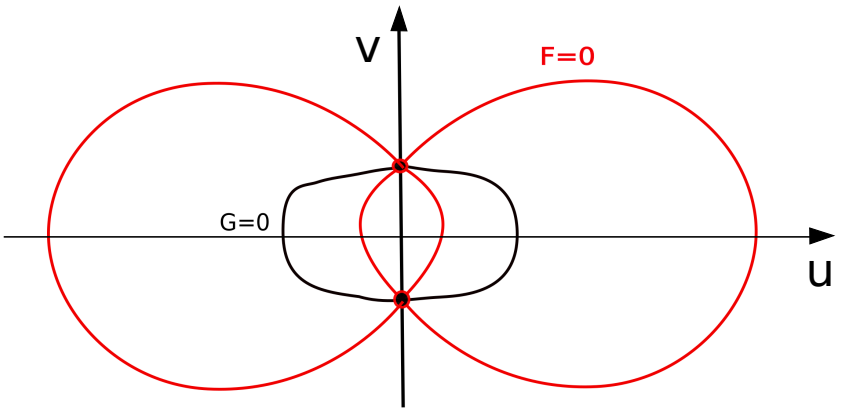

Figure 14: Level curves $F = 0$ (red) and $G = 0$ (black).

Let a 3-periodic $P_1P_2P_3$ be parametrized by $P_1(t) = (a\cos t, b\sin t)$, with $P_2(t)$ and $P_3(t)$ given in Appendix B. Using the trilinear coordinates above, we have $X_{162}(t) = (x_{126}(t),\ y_{126}(t))$ at $t = \frac{\pi}{2}$, $P_1 = (0, b)$ and $X_{162}(\frac{\pi}{2}) = (0, b)$.

Solve $x'_{162}(t)|_{t=\frac{\pi}{2}} = 0$ for a/b. After some long algebraic symbolic manipulation, this is equivalent to solving $5x^8 + 3x^6 - 32x^4 + 52x^2 - 36 = 0$, whose positive roots is $\alpha_{162} \simeq 1.16369$. □

Since $\alpha_{88} > \alpha_{162}$, setting $a/b > \alpha_{88}$ implies both centers will move non-monotonically.

If the EB be a lake, their joint motion is a dance along its margins. Over a complete revolution of $P_1(t)$ around the EB, X_{88} and X_{162} wind thrice around it, however:

Proposition 14. *X_{88} and X_{162} never coincide, therefore their paths never cross each other.*

Proof. Consider an elementary triangle $P_1 = (-1, 0)$, $P_2 = (1, 0)$ and $P_3 = (u, v)$. Obtain cartesian coordinates for X_{88} and X_{162} using their trilinears (Propositions 11 and 13). The equation $X_{88} = X_{162}$ is given by two algebraic equations $F(u, v, s_1, s_2) = G(u, v, s_1, s_2) = 0$ of degree 17 with $s_1 = \sqrt{(u-1)^2 + v^2} = |P_3 - P_2|$ and $s_2 = \sqrt{(u+1)^2 + v^2} = |P_2 - P_1|$. Particular solutions of these equations are equilateral triangles with $P_3 = (0, \pm\sqrt{3})$. Analytic and graphic analysis reveals that the level curves $F = G = 0$ are as shown in Figure 14.

Therefore the equilateral triangle is the only one such that the triangle centers X_{88} and X_{162} are equal. It is well known that an equilateral billiard orbit occurs only when the billiard ellipse is a circle. This ends the proof. □

Their never-crossing joint motion as well as the instants when they come closest is illustrated in Figure 15.

These paths can also be viewed as non-intersecting loops on the torus shown in Figure 16. An animation of this intricate motion can be viewed in [23, PL#14] with triangle centers imagined as swans.

Though we lack a theory for non-monotonicity of EB-bound TCs X_i, we think it is ruled by at least the following aspects:

- When the 3-periodic is an isosceles, will X_i lie at the summit vertex or below the base?
- As the 3-periodic rotates about the EB, does X_i follow it or move counter to it?
- Can X_i be non-monotonic? For example, neither X_{100} nor X_{190} ever are. If so, what is the aspect ratio α_i which triggers it?

Still murky is how the above derive from the Trilinears which specify X_i. We refer the reader to an animation depicting the joint motion of 20-odd such centers [23, PL#15].

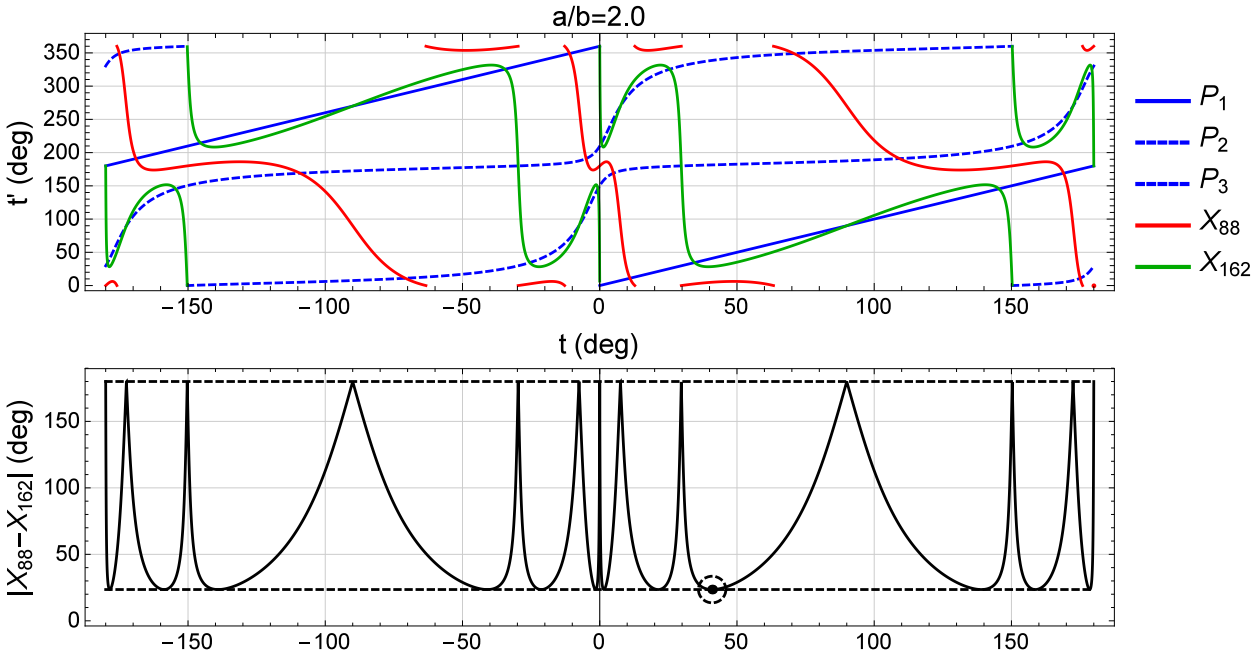

Figure 15: **Top**: location t' of 3-periodic vertices P_1 (blue), P_2 (dashed blue), and P_3 (dashed blue), as well as X_{88} (red), and X_{162}, plotted against the t parameter of $P_1(t)$. **Bottom**: absolute parameter difference along the EB between X_{88} and X_{162}. Notice there are 12 identical maxima at 180° occurring when the two centers at the left and right vertices of the EB. Additionally, there are 12 identical minima whose values can be obtained numerically. The fact that the minimum is above zero implies the points never cross. Note the highlighted minimum at $t\simeq 41°$: it is referred to in Figure 16.

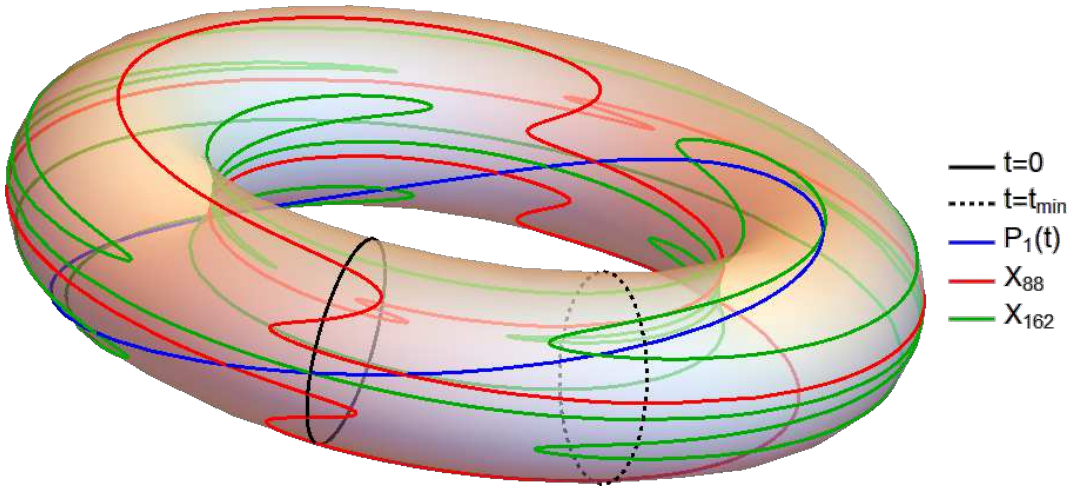

Figure 16: Visualizing the joint motion of $P_1(t), X_{88}, X_{162}$ on the surface of a torus. The meridians (circles around the smaller radius) correspond to a given t (a solid black meridian is wound at $t = 0$. The parallels represent a fixed location on the Billiard boundary. The curves for X_{88} and X_{162} are thrice-winding along the torus though never intersecting. To be determined: an analytic value for t where X_{88} and X_{162} are closest (there are 12 solutions). The dashed meridian represents one such minimum which for $a/b = 2$ occurs at $t \simeq 41°$. Notice it does not coincide with any critical points of motion.

4.4. Summary of phenomena

Tables 3 and 4 respectively summarize this section's various loci phenomena, and notable a/b thresholds.

Table 3: Loci phenomena for various Triangle Centers.

Point	*Type of Locus*	*Non-Monotonic*	*Comments*
X_{11}	Caustic	–	reverse dir.
Extouchpts.	Caustic	–	forward dir.
X_4	Upright Ellipse	–	Inside EB when $a < \alpha_4$
Orthic X_1	Can be 4-piece Ell.	–	If $a < \alpha_4$ is X_4 locus, else 4-piecewise ellipse: 2 arcs from X_4 locus, 2 arcs from EB
X_{26}	Can be non-compact	–	When $a/b \geq \alpha_4$, goes to ∞ if 3-periodic is right triangle
X_{40}	Upright Ellipse	–	At $a/b = \varphi$ identical to EB
X_{59}	At Least Sextic	–	4 Self-Intersections
X_{88}	EB	$a/b > \alpha_{88}$	at $a/b = \alpha_{88}^{\perp} > \alpha_4$ contains 3:4:5 triangle
X_{162}	EB	$a/b > \alpha_{162}$	never crosses X_{88}
ACT Intouchpts.	EB Boundary	$a/b > \alpha_{act}$	

Table 4: Aspect ratio thresholds, the degree of the polynomial used to find them, and their effects on loci phenomena.

symbol	a/b	Degree	*Significance*
α_{162}	1.164	8	above it, motion of X_{162} is non-monotonic
α_h	1.174	8	above it, some 3-periodic Orthics can be obtuse.
α_{act}	1.265	2	above it, motion of ACT Intouchpoints is non-monotonic
α_4	1.352	4	locus of X_4 is tangent to EB; above it, some 3-periodics are obtuse
$\alpha_{88}^{\perp}$	1.392	4	with X_{88} on a vertex, sidelengths are $3:4:5$
α_{88}	1.486	4	above it, motion of X_{88} is non-monotonic
α_4^*	1.510	6	X_4 locus identical to rotated EB
$\alpha_{59}^{\perp}$	1.580	–	when X_{59} is at self-intersection, 3-periodic is right triangle
φ	1.618	2	X_{40} locus identical to rotated EB

5. Conclusion

Examining the cygnine dynamic geometry and loci of 3-periodics under the prism of Classical Triangle Geometry has been productive. Surely additional secrets still hide under the EB's plumage. However, this haphazard experimental approach needs theoretical teeth. Toward that end, we submit the following questions to the reader:

- Can a Triangle Center be found such that its locus can intersect a straight line more than 6 times?
- The questions about X_{59} in Section 2.3.
- What causes a Triangle center to move monotonically (or not), forward or backward, with respect to the the monotonic motion of 3-periodic vertices?
- What is t in $P_1(t)$ at which point X_{88} or X_{162} reverses motion? When do they come closest?
- What can be said about the joint motion of other pairs in the 50+ list of EB-bound points provided in [14, X(9)]? Which are monotonic, which are not, is there a Pavlova or Baryshnikov amongst them?
- With [20] one observes X_{823} reverses direction at the exact moment a 3-periodic vertex crosses it. Can this be proven?

Videos mentioned herein are on a playlist [23], with links provided on Table 5. The reader is especially encouraged to interact with some of the above phenomena using our online applet [20]. A gallery of loci generated by X_1 to X_{100} (as well as vertices of derived triangles) is provided in [21].

Table 5: Videos mentioned in the paper. Column "PL#" indicates the entry within the playlist [23].

PL#	*Video Title*	*Section*
01	X_9 stationary at EB center	1
02	Loci for $X_1 \dots X_5$ are ellipses	1
03	Elliptic locus of Excenters similar to rotated X_1	1
04	Loci of X_{11}, X_{100} and Extouchpoints are the EB	1
05	Non-Ell. Loci of Medial, Intouch and Feuerbach Vertices	1
06	Pinning of Incenter of Orthic to Obtuse Vertex	2.1
07	Locus of Orthic Incenter is 4-piece ellipse	2.2
08	Locus of X_4, Orthic X_1, X_4, and Orthic's Orthic X_1	2.2
09	Non-monotonic motion on the EB of Anticompl. Intouchpoints	4.1
10	Locus of X_{88} is on the EB and can be non-monotonic	4.2
11	Non-monotonic motion of X_{88} and X_1X_{100} envelope	4.2
12	Locus of X_{59} with 4 self-intersections	2.3
13	Locus of X_{40} and the Golden Billiard	3.1
14	Swan Lake: the dance of X_{88} and X_{162}	4.3
15	Peter Moses' Points on the EB	4.3

Acknowledgements

Warm thanks go out to Clark KIMBERLING, PeterMOSES, Olga ROMASKEVICH, and Mark HELMAN for helpful discussions. The second autor is fellow of CNPq and coordinator of Project PRONEX/CNPq/FAPEG 2017 10 26 7000 508.

References

[1] A. AKOPYAN, R. SCHWARTZ, S. TABACHNIKOV: *Billiards in ellipses revisited.* URL https://arxiv.org/abs/2001.02934 (2020).

[2] M. BIALY, S. TABACHNIKOV: *Dan Reznik's identities and more.* URL https://arxiv.org/abs/2001.08469 (2020).

[3] H.S.M. COXETER, S.L. GREITZER: *Geometry Revisited.* New Mathematical Library, vol. 19, Random House, Inc., New York 1967.

[4] V. DRAGOVIĆ, M. RADNOVIĆ: *Caustics of Poncelet polygons and classical extremal polynomials.* Regul. Chaotic Dyn. **24**(1), 1–35 (2019). URL https://doi.org/10.1134/S1560354719010015

[5] C. FIEROBE: *On the circumcenters of triangular orbits in elliptic billiard.* URL https://arxiv.org/pdf/1807.11903.pdf (2018). Submitted

[6] R. GARCIA: *Elliptic billiards and ellipses associated to the 3-periodic orbits.* Amer. Math. Monthly **126**(06), 491–504 (2019). URL https://doi.org/10.1080/00029890.2019.1593087

[7] R. GARCIA, D. REZNIK: *Similar families: Poristic triangles and 3-periodics in the elliptic billiard.* URL https://arxiv.org/abs/2004.13509 (2020).

[8] R. GARCIA, D. REZNIK, J. KOILLER: *Loci of 3-periodics in an elliptic billiard: why so many ellipses?* URL https://arxiv.org/abs/2001.08041 (2020).

[9] R. GARCIA, D. REZNIK, J. KOILLER: *New properties of triangular orbits in elliptic billiards.* URL https://arxiv.org/abs/2001.08054 (2020).

[10] G. GLAESER, H. STACHEL, B. ODEHNAL: *The universe of conics. From the ancient Greeks to 21st century developments.* Springer Spektrum, Berlin 2016. URL https://doi.org/10.1007/978-3-662-45450-3.

[11] A. GLUTSYUK: *On curves with poritsky property.* arXiv (2019).

[12] M. HELMAN: *Locus of X_{88} and aspect ratio for $3:4:5$ 3-periodic.* Private Communication (January 2020).

[13] V. KALOSHIN, A. SORRENTINO: *On the integrability of Birkhoff billiards.* Phil. Trans. R. Soc. **A**(376) (2018). DOI https://doi.org/10.1098/rsta.2017.0419

[14] C. KIMBERLING: *Encyclopedia of triangle centers.* URL https://faculty.evansville.edu/ck6/encyclopedia/ETC.html (2019).

[15] C. KIMBERLING: *Polynomial triangle centers on the line at infinity.* J. Geom. **111**(10) (2020). URL 10.1007/s00022-020-0522-y

[16] V. LAZUTKIN: *The existence of caustics for a billiard problem in a convex domain.* Math. USSR Izvestija **7**, 185–214 (1973).

[17] M. LEVI, S. TABACHNIKOV: *The Poncelet grid and billiards in ellipses.* Amer. Math. Monthly **114**(10), 895–908 (2007). URL https://doi.org/10.1080/00029890.2007.11920482

[18] B. Odehnal: *Poristic loci of triangle centers.* J. Geometry Graphics **15**(1), 45–67 (2011).

[19] H. Poritsky: *The billiard ball problem on a table with a convex boundary – an illustrative dynamical problem.* Ann. of Math. **51**(2), 446–470 (1950).

[20] D. Reznik: *Applet showing the locus of several triangular centers.* URL https://editor.p5js.org/dreznik/full/i1Lin7lt7 (2019).

[21] D. Reznik: *Loci of triangle centers x(1)–x(100): Orbits and 6 derived triangles.* URL https://bit.ly/2TCsHFU (2019).

[22] D. Reznik: *YouTube playlist for mathematical intelligencer.* URL https://bit.ly/2kTvPPr (2019).

[23] D. Reznik: *Playlist for "Loci of Triangular Orbits in an Elliptic Billiard: Intriguing Phenomena".* URL https://bit.ly/2vvJ9hW (2020).

[24] D. Reznik, R. Garcia, J. Koiller: *Can the elliptic billiard still surprise us?* Math. Intelligencer **42** (2019). URL https://rdcu.be/b2cg1

[25] O. Romaskevich: *On the incenters of triangular orbits on elliptic billiards.* Enseign. Math. **60**(3-4), 247–255 (2014). URL https://arxiv.org/pdf/1304.7588.pdf

[26] U.A. Rozikov: *An Introduction To Mathematical Billiards.* World Scientific Publishing Company, 2018.

[27] S. Tabachnikov: *Geometry and Billiards.* Student Mathematical Library vol. 30, American Mathematical Society, Providence, RI 2005. URL http://www.personal.psu.edu/sot2/books/billiardsgeometry.pdf

[28] S. Tabachnikov: *Projective configuration theorems: old wine into new wineskins.* In: S. Dani, A. Papadopoulos (eds.): [*Geometry in History*, Springer Verlag 2019, pp. 401–434. URL https://arxiv.org/pdf/1607.04758.pdf

[29] J.H. Weaver: *Invariants of a poristic system of triangles.* Bull. Amer. Math. Soc. **33**(2), 235–240 (1927). URL https://doi.org/10.1090/S0002-9904-1927-04367-1

[30] E. Weisstein: *Mathworld.* URL http://mathworld.wolfram.com (2019).

[31] P. Yiu: *Conic construction of a triangle from its incenter, nine-point center, and a vertex.* J. Geometry Graphics **16**(2), 171–183 (2012).

A. Obtuse triangles and their orthics

Let $T = ABC$ be any triangle and $T' = A'B'C'$ its Orthic (Figure 2). Let X_1' be the orthic's Incenter.

Lemma 2. *If T is acute, the Incenter X_1' of T' is the Orthocenter X_4 of T.*

Proof. This is Fagnano's Problem, i.e., the Orthic is the inscribed triangle of minimum perimeter, and the altitudes of T are its bisectors [26, Section 3.3]. Since the altitudes or T are bisectors of T' this completes the proof. □

Lemma (1). *If T is obtuse, the Incenter X_1' of T' is the vertex of T subtending the obtuse angle.*

Proof. Let B be the obtuse angle. Then B' will be on the longest side of T whereas A' (resp. C') will lie on extensions of BC (resp. AB), i.e., A' and C' are exterior to T. Therefore, X_4 will be where altitudes AA' and CC' meet, also exterior to T. Since $AA' \perp CB$ and $CC' \perp AB$, then CA' and AC' are altitudes of triangle $T_e = AX_4C$. Since these meet at B, the latter is the Orthocenter of T_e and $T' = A'B'C'$ is its Orthic, noting that the pre-image of T' comprises both T and T_e. By Lemma 2, lines CA', AC', X_4B' are bisectors of T', therefore their meetpoint B is the Incenter of T'. □

Corollary 1. *When T is obtuse, $T_e = AX_4C$ is acute and the Excentral Triangle of T'.*

Since all vertices of T' lie on the sides of T_e, this is the situation of Lemma 2, i.e., T_e is acute. Notice the sides of T_e graze each vertex of T' perpendicular to the bisectors, which is the construction of the Excentral Triangle.

Let Q be a generic triangle and Q_e its Excentral [30]. Let θ_i be angles of Q and ϕ_i those of Q_e opposite to the θ_i's. By inspection, $\phi_i = \frac{\pi - \theta_i}{2}$, i.e., all excentral angles are less than $\pi/2$.

Corollary 2. *Cor.2 If T is obtuse, X_4 is an Excenter of T'* [3].

X_4 is the intermediate vertex of T_e.

B. 3-Periodic vertices

Results here were first derived in [6]. The EB semi-axes are $a > b > 0$. Let $P_i = (x_i, y_i)$ denote the 3-periodic vertices, $i = 1, 2, 3$, and α denote the angle of incidence (and reflection) with respect to the Elliptic Billiard normal at P_1. This is given by:

$$\cos\alpha = \frac{a^2 b\sqrt{-a^2 - b^2 + 2\sqrt{a^4 - b^2c^2}}}{c^2\sqrt{a^4 - c^2x_1^2}},$$

where $c = \sqrt{a^2 - b^2}$. Parametrize $P_1 = (a\cos t,\, b\sin t)$. Coordinates $x_2 = \frac{p_{2x}}{q_2}$ and $y_2 = \frac{p_{2y}}{q_2}$ are given by:

$$\begin{aligned}
p_{2x} =& -b^4\left(\left(a^2+b^2\right)\cos^2\alpha - a^2\right)x_1^3 - 2a^6\,\cos\alpha\sin\alpha\,y_1^3\\
&+ a^4\left(\left(a^2-3\,b^2\right)\cos^2\alpha + b^2\right)x_1\,y_1^2 - 2\,a^4b^2\cos\alpha\,\sin\alpha x_1^2 y_1,\\
p_{2y} =& 2b^6\,\cos\alpha\sin\alpha\,x_1^3 - a^4\left(\left(a^2+b^2\right)\cos^2\alpha - b^2\right)y_1^3\\
&+ 2\,a^2b^4\cos\alpha\sin\alpha\,x_1y_1^2 + b^4\left(\left(b^2-3\,a^2\right)\cos^2\alpha + a^2\right)x_1^2y_1\\
q_2 =& b^4\left(a^2 - \left(a^2-b^2\right)\cos^2\alpha\right)x_1^2 + a^4\left(b^2 + \left(a^2-b^2\right)\cos^2\alpha\right)y_1^2\\
&- 2\,a^2b^2\left(a^2-b^2\right)\cos\alpha\sin\alpha\,x_1\,y_1.
\end{aligned}$$

Likewise, $x_3 = \frac{p_{3x}}{q_3}$ and $y_3 = \frac{p_{3y}}{q_3}$ are given by:

$$\begin{aligned}
p_{3x} =& b^4\left(a^2 - \left(b^2+a^2\right)\right)\cos^2\alpha x_1^3 + 2\,a^6\cos\alpha\,\sin\alpha\,y_1^3\\
&+ a^4\left(\cos^2\alpha\left(a^2-3\,b^2\right) + b^2\right)x_1\,y_1^2 + 2\,a^4b^2\cos\alpha\sin\alpha\,x_1^2y_1\\
p_{3y} =& -2\,b^6\cos\alpha\sin\alpha\,x_1^3 + a^4\left(b^2 - \left(b^2+a^2\right)\cos^2\alpha\right)\,y_1^3\\
&- 2\,a^2b^4\cos\alpha\sin\alpha\,x_1y_1^2 + b^4\left(a^2 + \left(b^2-3\,a^2\right)(\cos\alpha)^2\right)x_1{}^2y_1,\\
q_3 =& b^4\left(a^2 - \left(a^2-b^2\right)\cos^2\alpha\right)x_1^2 + a^4\left(b^2 + \left(a^2-b^2\right)\cos^2\alpha\right)y_1^2\\
&+ 2\,a^2b^2\left(a^2-b^2\right)\cos\alpha\sin\alpha\,x_1\,y_1.
\end{aligned}$$

Received March 24, 2020; final form May 5, 2020